Type 1 fimbriae-mediated collective protection against type 6 secretion system attacks

Margot Marie Dessartine, Artemis Kosta, Thierry Doan, Éric Cascales, Jean-Philippe Côté

AMERICAN SOCIETY FOR MICROBIOLOGY | mBio

| Bacteriology | Research Article

Type 1 fimbriae-mediated collective protection against type 6 secretion system attacks

Margot Marie Dessartine,[1] Artemis Kosta,[2] Thierry Doan,[3] Éric Cascales,[3] Jean-Philippe Côté[1]

AUTHOR AFFILIATIONS See affiliation list on p. 14.

ABSTRACT Bacterial competition may rely on secretion systems such as the type 6 secretion system (T6SS), which punctures and releases toxic molecules into neighboring cells. To subsist, bacterial targets must counteract the threats posed by T6SS-positive competitors. In this study, we used a comprehensive genome-wide high-throughput screening approach to investigate the dynamics of interbacterial competition. Our primary goal was to identify deletion mutants within the well-characterized *E. coli* K-12 single-gene deletion library, the Keio collection, that demonstrated resistance to T6SS-mediated killing by the enteropathogenic bacterium *Cronobacter malonaticus*. We identified 49 potential mutants conferring resistance to T6SS and focused our interest on a deletion mutant (Δ*fimE*) exhibiting enhanced expression of type 1 fimbriae. We demonstrated that the presence of type 1 fimbriae leads to the formation of microcolonies and thus protects against T6SS-mediated assaults. Collectively, our study demonstrated that adhesive structures such as type 1 fimbriae confer collective protective behavior against T6SS attacks.

IMPORTANCE Type 6 secretion systems (T6SS) are molecular weapons employed by gram-negative bacteria to eliminate neighboring microbes. T6SS plays a pivotal role as a virulence factor, enabling pathogenic gram-negative bacteria to compete with the established communities to colonize hosts and induce infections. Gaining a deeper understanding of bacterial interactions will allow the development of strategies to control the action of systems such as the T6SS that can manipulate bacterial communities. In this context, we demonstrate that bacteria targeted by T6SS attacks from the enteric pathogen *Cronobacter malonaticus*, which poses a significant threat to infants, can develop a collective protective mechanism centered on the production of type I fimbriae. These adhesive structures promote the aggregation of bacterial preys and the formation of microcolonies, which protect the cells from T6SS attacks.

KEYWORDS bacterial competition, type 6 secretion system, Keio collection, microcolony formation, type 1 fimbriae

Bacteria are often found within complex microbial communities where constant interactions occur. Effective competition strategies are essential for survival, especially in environments where nutrients and micro-elements (e.g., iron) are limited (1). For instance, some microorganisms secrete antimicrobial molecules targeting surrounding microbes (2). In bacteria, competitive interactions are often mediated by secretion systems (3, 4). Secretion systems are protein complexes that allow the passage of proteins across the cell envelope and are involved in bacterial virulence by promoting the invasion of eukaryotic cells or scavenging resources in the environment (5, 6). Twelve secretion systems have been identified in bacteria. Among them, the type 6 secretion system (T6SS) is a potent weapon that delivers toxins into surrounding bacterial cells (7, 8). The T6SS also contributes to virulence by driving the remodeling of microbial

Editor Matthew R. Chapman, University of Michigan-Ann Arbor, Ann Arbor, Michigan, USA

Address correspondence to Jean-Philippe Côté, jp.cote@usherbrooke.ca.

The authors declare no conflict of interest.

See the funding table on p. 14.

Received 27 September 2023
Accepted 25 January 2024
Published 18 March 2024

communities by pathogenic bacteria and facilitating the establishment of T6SS-positive pathogens (9–11).

The T6SS is a harpoon-like contractile nanomachine that triggers interbacterial competition through the injection of toxic effectors directly into target cells in a contact-dependent manner (12, 13). This nano-harpoon is composed of a membrane complex and a baseplate that serves as a docking station for the assembly of a tail tube/sheath complex (14–16). The tail tube is composed of stacked Hcp hexamers wrapped by a sheath formed by the TssB and TssC proteins (17, 18). The tube is capped by the spike, comprising the VgrG trimer sharpened with the PAAR-domain protein (19). Effector proteins displaying diverse functions [phospholipases (20), amidases (21), DNases (22), etc.] (23) can be loaded within the lumen of the Hcp tube or linked as cargo to VgrG/PAAR domain proteins directly or with the support of specific adaptors (12, 24, 25). The sheath is polymerized in an extended conformation, and upon its contraction, the tail tube is pushed across the envelope of both attacker and target cells, so the antibacterial T6SS effectors can be delivered directly into target cells to kill them.

Target cells can display defense mechanisms against T6SS attacks. The main defense system is orchestrated by immunity proteins that usually specifically bind to the effectors (13). This approach is also used by attacker cells to avoid autointoxication. Immunity-independent resistance to T6SS has also been reported. Indeed, *Escherichia coli* can sense T6SS effectors through envelope stress-response pathways and resists T6SS attacks from *Vibrio cholerae* (26). Moreover, target cells can modulate environmental parameters influencing the interaction between attacker and target cells. For example, introducing spatial separation between target and attacker cells is an effective mechanism of resistance to contact-dependent attacks by T6SS (27, 28). This spatial segregation may be due to the production of exopolysaccharides (EPS) to form a physical barrier (29) or biofilm formation (30) which can lead to the formation of microcolonies protecting cells located at the center, by the formation of a barrier of dead cells and debris at the attacker-target interface (28, 31). Collective behaviors are widespread in microbial environment, such as the intestinal microbiota (32, 33), where T6SS performs crucial functions to modulate population dynamics between host-associated microbes, enteric pathogens, and host immune response (34, 35). Despite growing interest in resistance mechanisms, many aspects remain unknown regarding target cell defenses against T6SS assaults.

High-throughput approaches using ordered libraries of mutants allow to rapidly discover and investigate new genetic pathways involved in a phenotype of interest (36, 37), including the regulation of T6SS (38). In this study, we developed a screening method that enabled us to analyze interbacterial competition in a genome-wide high-throughput manner. Using *Cronobacter malonaticus,* an *Enterobacteria* highly prevalent in powdered infant formula and known to cause severe infections in newborns and immunocompromised individuals (e.g., meningitis, necrotizing enterocolitis) (39), as a model attacker bacterium, and the single-gene deletion mutants for all nonessential *E. coli* K-12 genes library (Keio collection) (40) as target cells, we identified that the deletion of the *fimE* recombinase provides resistance to T6SS attacks. We further showed that a Δ*fimE* mutant overexpressed type 1 fimbriae leading to the formation of microcolonies. Target cells within these microcolonies were protected from contact-dependent killing mediated by the T6SS, leading to their survival. This defense mechanism could represent a nonspecific resistance mechanism, unlike immunity proteins, which could potentially lead to resistance against a broad range of assailants.

RESULTS

Cronobacter malonaticus 3267 efficiently kills *E. coli* in a T6SS-dependent manner

A recent study has shown that a conserved T6SS gene cluster among *Cronobacter sakazakii* strains displays a strong activity in laboratory conditions (41). Based on this study, we hypothesized that *Cronobacter malonaticus* strain 3267 may also possess

a functional T6SS. Sequencing confirmed the presence of a T6SS gene cluster in *C. malonaticus* 3267, bearing similarities to the T6SS-1 found in *C. sakazakii* ATCC 12868 (Fig. 1A). A bacterial competition assay validated that *C. malonaticus* 3267 displays antibacterial activity against *E. coli* in typical laboratory growth conditions (Fig. 1B). We used *E. coli* BW25113 Δ*yejO* from the Keio collection as target cells, which we consider as wild-type (WT) *E. coli* in our study. *yejO* is a pseudogene in *E. coli*, inactivated by an insertion sequence (IS5K) close to its start codon. BW25113 Δ*yejO* target is eliminated to a similar extent than *E. coli* BW25113 WT strain, thus making it a suitable target cell in our study (Fig. S1A).

To test whether the antibacterial activity of *C. malonaticus* was T6SS dependent, we quantified the survival of *E. coli* Δ*yejO* target cells after co-incubation with a WT or a T6SS-inactive mutant of *C. malonaticus* 3267 (Δ*tssM*). When *E. coli* Δ*yejO* is incubated with WT *C. malonaticus* 3267, ~5×10^4 CFUs of target cells were recovered after the competition assay (Fig. 1B and C). However, when co-incubated with the Δ*tssM* mutant, ~1×10^{12} CFUs of target cells were recovered. The deletion of *tssM* did not affect the growth of *C. malonaticus* 3267 (Fig. S1B), and the presence of target cells did not affect *C. malonaticus* 3267 (Fig. S1C). Collectively, these data suggest that *C. malonaticus* 3267 employs its T6SS to eliminate *E. coli* target cells.

A high-throughput interbacterial competition assay identifies *E. coli* Δ*fimE as* resistant to T6SS

High-throughput interbacterial competition (HTIC) assays combined with the use of target or attacker libraries of mutants are effective in uncovering new mechanisms involved in T6SS function and biogenesis (38). We performed a high-throughput competition assay between the Keio collection mutants as target cells and *C. malonaticus* 3267 as the attacker strain (Fig. 2A). We co-cultured targets and attackers on competition plates in a 1,536-colony density format. After 24 h of co-incubation, colonies were replicated on selection plates containing kanamycin, allowing the growth of the Keio mutants that escaped T6SS killing. We expected that the deletion of genes related to T6SS susceptibility would increase survival of prey cells upon interbacterial competition.

To avoid bias in determining which genes confer resistance to the T6SS attack, we used binary values, where 1 means growth and 0 means no growth, instead of measuring colony size or colony density. Keio mutants can display different colony morphologies (e.g., small, mucoid, and sticky) (42), and therefore, measuring colony size on the selection plates does not correlate with the resistance level of target cells. The binary values of three replicates were averaged in order to score the mutants in the Keio collection (Fig. 2B).

Of the ~4,000 Keio mutants, only 49 displayed resistance (Table S2) to T6SS in at least two out of the three replicates as some defense mechanisms can provide only partial resistance to T6SS (27). These resistant mutants included the *fimE* mutant. In pairwise interbacterial competition assays against the WT attacker, the *fimE* mutant displayed a difference of almost 4 log CFUs in survival compared to the *yejO* mutant (Fig. 2C). However, the *fimE* mutant still showed lower survival than target cells in competition with the Δ*tssM* attacker (~4 log CFUs), suggesting that the *fimE* mutant conferred only partial resistance to T6SS attacks (Fig. 2C). Transcomplementation using the high-copy pCA24N-*fimE* plasmid (43) restored the killing by *C. malonaticus* 3267 to WT levels (Fig. 2D), confirming that the observed phenotype is the result of the deletion of the *fimE* gene.

E. coli BW25113 Δ*fimE* exhibits increased production of type 1 fimbriae

The *fim* operon is composed of nine genes encoding structural, assembly, and transport components (*fimAICDFGH*) as well as regulators (*fimB* and *fimE*). FimA is the major structural subunit of the fimbriae and is secreted by the FimC chaperone and the FimD usher (44). FimH encodes a mannose-specific adhesin located at the tip of the fimbriae that mediates the attachment to mannosylated receptors at the cell surface. FimB and

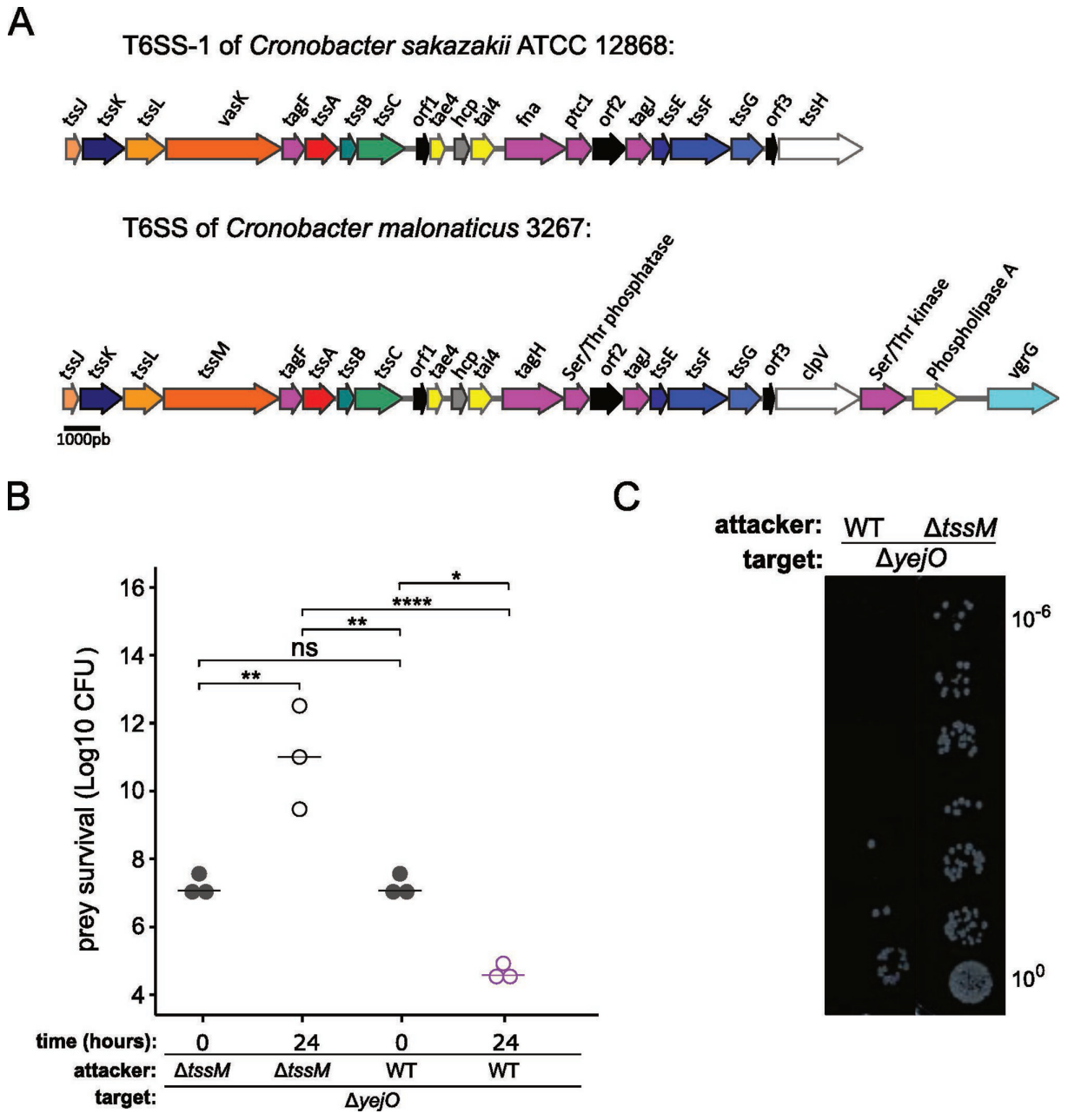

FIG 1 *C. malonaticus* 3267 kills *E. coli* BW25113 in a T6SS-dependent manner. (A) Schematic representation of the T6SS-1 gene cluster in *C. sakazakii* ATC12868 (from Wang et al. [41]) and of the T6SS gene cluster in *C. malonaticus* 3267. Structural genes of the membrane complex are displayed in light to dark orange. Genes coding for baseplate proteins are displayed in light to dark blue. The genes *tssB* and *tssC* of the tail tube/sheath complex are shown in light and dark green. Genes coding for proteins involved in T6SS post translational regulation are indicated in pink. Genes coding for toxins and antitoxins are displayed in yellow. Open reading frame with unknown function is shown in black. (B) Attackers and kanamycin-resistant target cells were mixed at a concentration of 10^6 CFU and at a ratio of 1:1 and incubated onto a nitrocellulose filter for 24 h. Surviving target cells at 0 and 24 h were enumerated by plating on selective agar plates. Target survival is presented in log10 CFUs. (C) Representative picture of the target cells selection after the killing assay. One-way ANOVA test was performed to determine statistical significance (ns = nonsignificant, *$P \leq 0.05$, **$P \leq 0.005$, ****$P \leq 0.0001$). Data represent three independent experiments.

FimE encode recombinases that control the permutation of an invertible 314 bp element (*fim* switch) located directly in front of *fimA* and flanked by two inverted 9 bp repeats (45, 46). This inversion activates or prevents the transcription of type 1 fimbriae genes in a process called phase variation (47). The FimE recombinase preferentially switches from a phase with fimbriae production (ON-phase) to a phase without fimbriae production

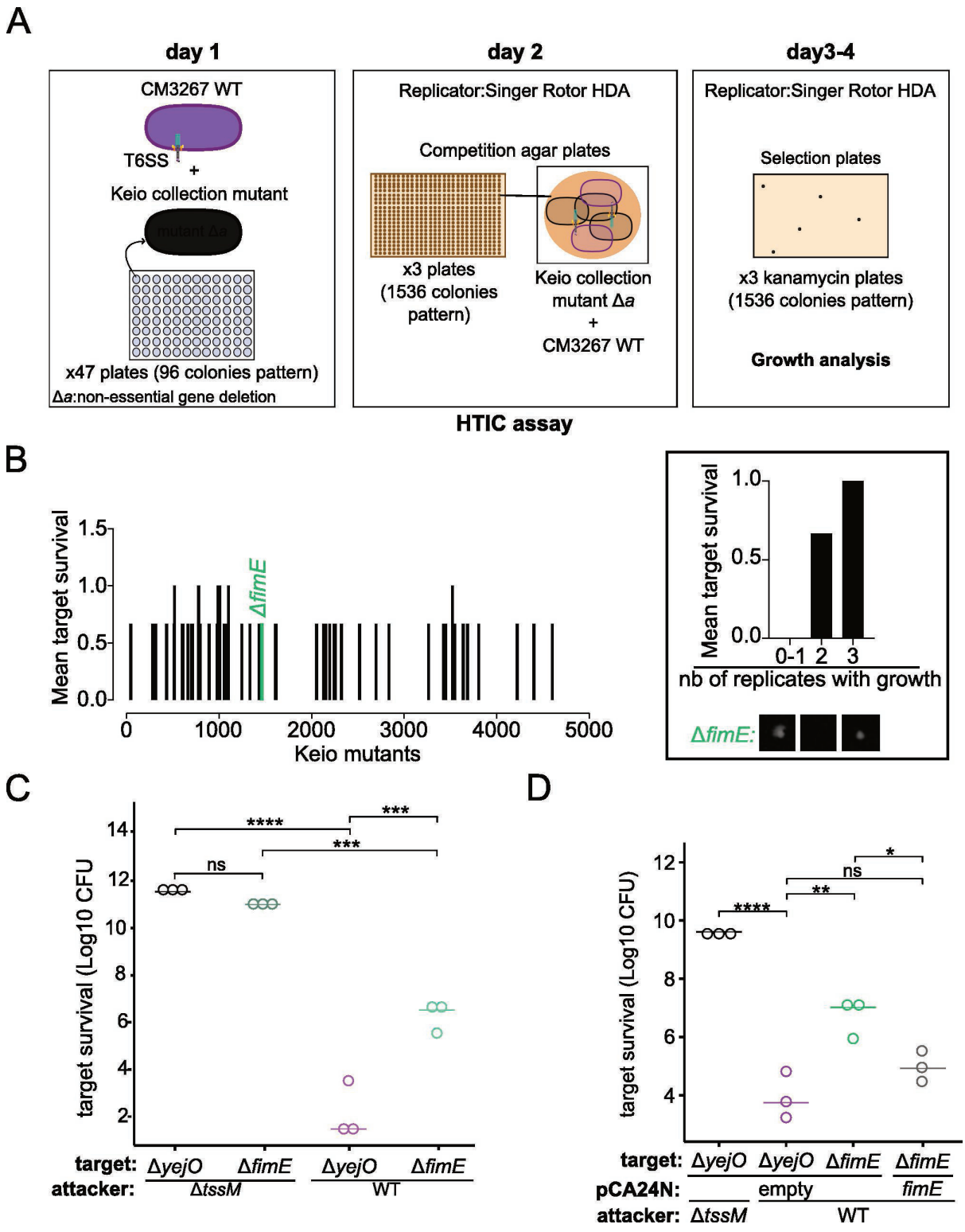

FIG 2 High-throughput interbacterial competition assay identifies *E. coli* BW25113 Δ*fimE* mutant as resistant to *C. malonaticus* 3267 T6SS-mediated killing. (A) Schematic representation of the HITC assay methodology (CM3267: *C. malonaticus* 3267). (B) Bar plot of mutant survival after the HTIC assay. For each replicate, survival was assessed using binary value; colony growth = 1, no colony growth = 0. In this setting, a mutant is resistant if there is a surviving colony in at least two of the three replicates. (C) Interbacterial competition assay between WT or Δ*tssM* attackers and Δ*yejO* or Δ*fimE* target cells. (D) Complementation of Δ*fimE* mutant with pCA24N plasmid (empty vector or *fimE*) to restore the susceptibility to T6SS. (C and D) Target survival is presented in log10 CFU. One-way ANOVA test was performed to determine statistical significance (ns = nonsignificant, **P* ≤ 0.05, ***P* ≤ 0.005, ****P* ≤ 0.0005, *****P* ≤ 0.0001). Data represent three independent experiments.

(OFF-phase), whereas FimB recombinase mediates permutations in both directions, with a preference to an ON-phase orientation (48, 49).

The overall effect of the FimE recombinase on the expression of fimbriae is still debated. Orndorff et al. demonstrated an increase in the number of fimbriae per cell in *E. coli* when producing the *fim* operon from a high copy number plasmid containing a deletion of the *fimE* gene (50). However, another study showed no difference in bacterial fimbriation in the isogenic *fimE* mutant in *E. coli* MG1655 compared to the WT strain (51). Therefore, we first analyzed the production of type 1 fimbriae of the *E. coli* BW25113 *fimE* mutant. Electron microscopy revealed that 50% of the Δ*fimE* cells possessed fimbriae compared to only 15% of Δ*yejO* cells (Fig. 3A and B). Moreover, when Δ*fimE* cells were fimbriated, there were more fimbriae per cell, with 33% of cells having more than 15 fimbriae on their surface, compared to only 1.4% of Δ*yejO* cells (Fig. 3B).

We also observed that when centrifuged, the *fimE* mutant formed aggregates that did not dissociate easily. Shear stress is known to enhance the adhesion of bacteria via the FimH adhesin of type 1 fimbriae (52). Therefore, we next observed by microscopy if the increased production of type 1 fimbriae in the *fimE* mutant led to the formation of microcolonies (Fig. 3C). Bacterial cultures were centrifuged and vortexed, then spotted onto semi-solid Luria broth (LB) agar, and observed on a confocal microscope. Only the *fimE* deletion mutant was able to form large microcolonies. The area of all particles was analyzed to assess the size of microcolonies (Fig. 3D). Δ*fimE* strain had a significantly greater average particle size compared to the Δ*yejO* strain (Fig. 3E). The observed variability within the size of microcolonies for Δ*fimE* strains correlates with the electron microscopy findings, showing that 50% of cells produce fimbriae. Overall, these results show that the *fimE* deletion mutant actively produces type 1 fimbriae and forms microcolonies when subjected to shear forces.

Type 1 fimbriae mediate the formation of microcolonies

We next investigated whether the formation of microcolonies was linked to the FimH adhesin located at the tip of the type 1 fimbrial structure. Our goal was to determine whether the microcolonies were responsible for the resistance to T6SS attacks or whether the fimbriae themselves were sufficient to obstruct T6SS assaults. Because of their length (~1 µm) and their considerable number on the cell surface (>200/cell) (44, 53), type 1 fimbriae could mask direct interactions between cell structures and the environment. One possibility is thus that fimbriated cells are shielded against T6SS by the fimbriae covering their surface.

To confirm that the formation of microcolonies observed was mediated by type 1 fimbriae, we next observed the formation of microcolonies in the *fimE* mutant with (5%) and without D-mannose (Ctrl) (Fig. 4A). D-mannose binds the FimH adhesin at the tip of type 1 fimbriae inhibiting adhesion (54) and agglutination to yeast (55). Indeed, we observed that adding D-mannose to the *fimE* mutant bacterial cultures inhibited the formation of microcolonies (Fig. 4A). The Δ*fimE* strain supplemented with D-mannose led to the reduction of the size of particles in comparison to the Δ*fimE* mutant without D-mannose (Fig. 4C). The analysis of particle sizes across multiple experiments further showed that the Δ*fimE* strain had a significantly greater average particle compared to the Δ*fimE* mutant supplemented with D-mannose (Fig. 4D).

In addition, type 1 fimbriated cells are known to promote yeast agglutination (55). Overnight cultures of various bacterial strains were mixed with rehydrated *Saccharomyces cerevisiae*, spotted on a glass slide, and observed macroscopically. As expected, *E. coli* Δ*yejO* did not agglutinate *S. cerevisiae* cells (Fig. 4B) in contrast to the solution containing the *fimE* mutant where agglutination was visible. The agglutination phenotype observed with the *fimE* mutant was inhibited by the addition of D-mannose, as expected.

Finally, we tested whether functional (i.e., adhesive) type 1 fimbriae were needed to promote resistance to T6SS-mediated killing. Therefore, we performed the competition assay in the presence or absence of D-mannose (Fig. 4E). As observed previously, the *fimE* mutant was protected against T6SS attacks. The addition of D-mannose to Δ*fimE* cultures

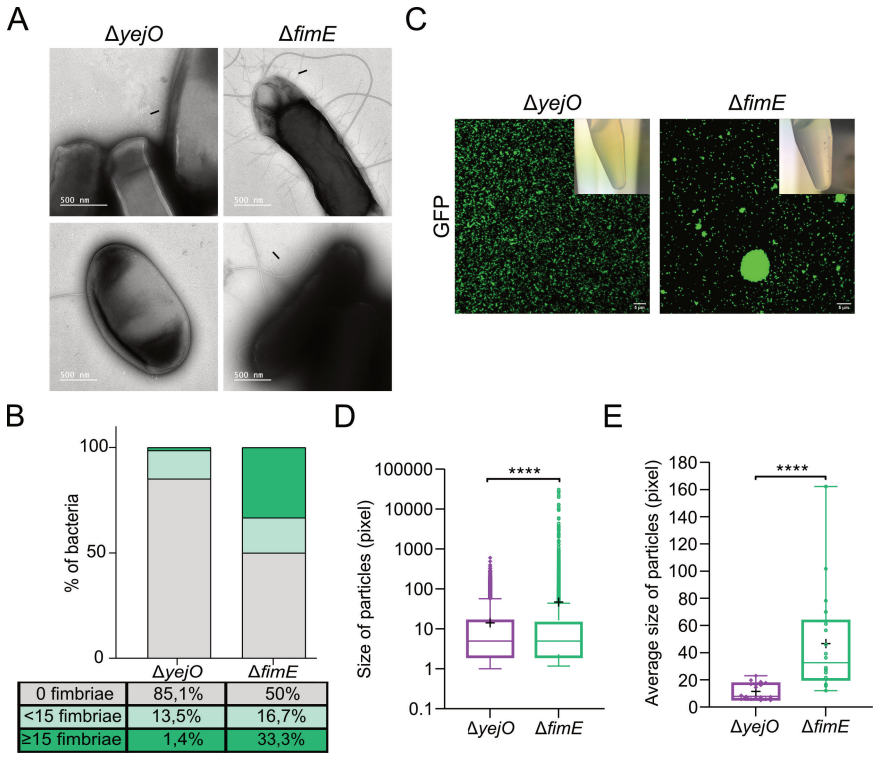

FIG 3 The Δ*fimE* mutant produces type 1 fimbriae that promote the formation of bacterial microcolonies. (A) Electron microscopy of fimbriated cells. Negatively stained preparation of a 24-h stationary culture of *E. coli* BW25113 Δ*yejO* and Δ*fimE*, grown on Luria Broth agar plate. (B) Proportion of fimbriated and nonfimbriated cells in Δ*yejO* (n = 74; 14.9% of fimbriated cells) and Δ*fimE* (n = 60; 50% of fimbriated cells). (C) gfp-Expressing strains were spotted in duplicate after centrifugation and vortex cycle and observed in fluorescence microscopy. Three images were taken at random points for each duplicate for three independent experiments. Microcolonies size was assessed using ImageJ. (D) Box plot of the particle sizes of the Δ*yejO* and Δ*fimE* mutants. Box plots extend from the 5th to 95th percentiles. Cross, mean; crossing line, median. Nonparametric Mann Whitney test was performed to determine statistical significance (****P < 0.0001). (E) Box plot of the average size of particles of each random point images (n = 18). Unpaired t-test was performed to determine statistical significance (****P < 0.0001). Box plots extend from the minimum to the maximum, showing all points. Cross, mean; crossing line, median.

to prevent the formation of microcolonies led to the loss of T6SS resistance to the same extent as the Δ*yejO* strain (Fig. 4E). In these conditions, growth of *C. malonaticus* and T6SS activity are not affected by the addition of 5% of D-mannose (Fig. S2A and B). We also performed the same experiments using a double *fimE fimH* deletion mutant and observed similar results (Fig. S3). Collectively, these findings highlight the implication of FimH adhesive interactions in the formation of microcolonies and resistance to T6SS-mediated killing. In addition, the interbacterial killing assays suggest that T6SS resistance exhibited by the *fimE* mutant is not due to single-cell spatial segregation driven by the fimbriae but more likely attributed to microcolonies formed through FimH.

Formation of microcolonies by type 1 fimbriated target cells leads to their resistance to the T6SS

We have shown that D-mannose inhibited microcolony formation and suppressed the resistance to T6SS-mediated attacks. However, about 50% of the Δ*fimE* cells expressed type 1 fimbriae. In addition, the *fimE* deletion does not grant a complete resistance to T6SS attacks. Thus, we hypothesized that target cells inside microcolonies are protected, while individual cells are killed by the attacker. To test our hypothesis, we performed a

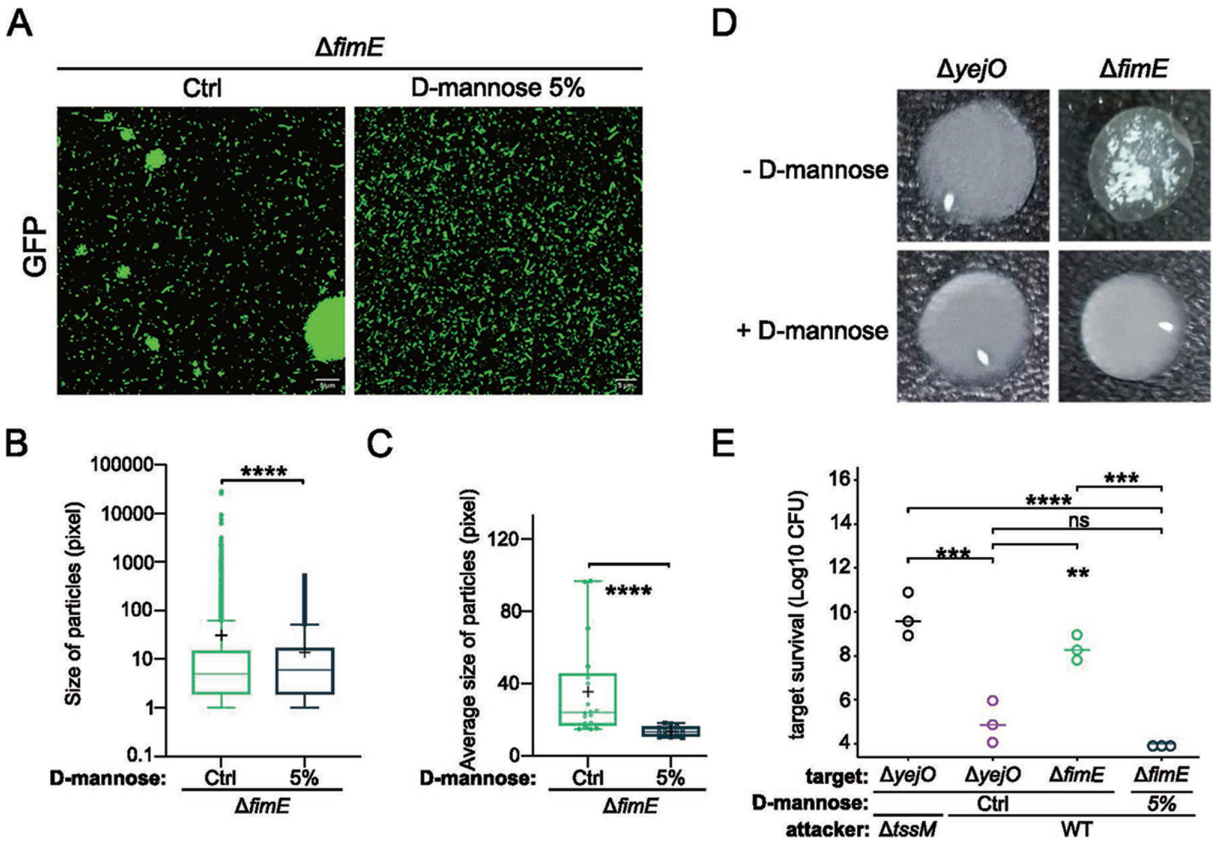

FIG 4 Type 1 fimbriae adhesin is essential for microcolony formation and T6SS resistance. (A) Visualization of microcolonies using fluorescence microscopy. (B) Yeast agglutination assay with and without D-mannose (competitive ligand binding to FimH). Agglutination phenotype is observed for the Δ*fimE* mutant. The absence of agglutination is characterized by a cloudy appearance of the mixture. (C) Box plot of the overall size of particles distribution of the Δ*fimE* mutant with and without 5% of D-mannose. Box plots extend from the minimum to the maximum, showing all points. Cross, mean; crossing line, median. Nonparametric Mann Whitney tests were performed to assess statistical significance using R (****$P \leq 0.0001$). (D) Box plot of the average size of particles of each random point images ($n = 18$). Box plots extend from the 5th to 95th percentiles. Cross, mean; crossing line, median. Unpaired *t*-test was performed to assess statistical significance using R (**$P = 0.005$). (E) Interbacterial competition assay between WT or Δ*tssM* attackers and Δ*yejO* or Δ*fimE* (with and without 5% of D-mannose) target cells. Target survival after killing assays is presented in log10 CFUs. One-way ANOVA test was used followed by Tukey post hoc test to determine statistical significance using R (ns = nonsignificant, **$P \leq 0.005$, ***$P \leq 0.0005$, ****$P \leq 0.0001$). Data represent three independent experiments.

time course interbacterial competition assay adapted from Granato et al. (29). Co-cultures were spotted directly onto LB-agar in 12-well plates and imaged every hour for 6 h to observe the GFP-positive target cells (Fig. 5A). The susceptibility of GFP-negative and GFP-positive target cells to T6SS killing was similar (Fig. S4). The total fluorescence inside the spot was then evaluated at 0 and 6 h (Fig. 5B), where the fluorescence intensity represents a measurement of target cells survival. When grown with a T6SS-deficient attacker, the Δ*yejO* target strain multiplied strongly as expected, reaching a 10-fold higher fluorescence intensity ratio at 6 h compared with T_0. On the other hand, the Δ*yejO* target strain was eliminated after 6 h of co-culture with the T6SS-positive attacker. We observed the same result for the Δ*fimE* target supplemented with 5% of D-mannose, validating our previous assertions that the fimbrial structure by itself is not sufficient to confer resistance to T6SS. In condition without D-mannose supplementation, the Δ*fimE* mutant was found within microcolonies as well as single cells (i.e., weak fluorescence signal across the entire spot) at T_0. Here, however, cells found in microcolonies survived the T6SS attack, while the fluorescence signal from the single cells was not detectable at 6 h. Overall, our results suggest that cells inside type 1 fimbriae-mediated microcolonies are protected from T6SS attacks, while individual cells are not.

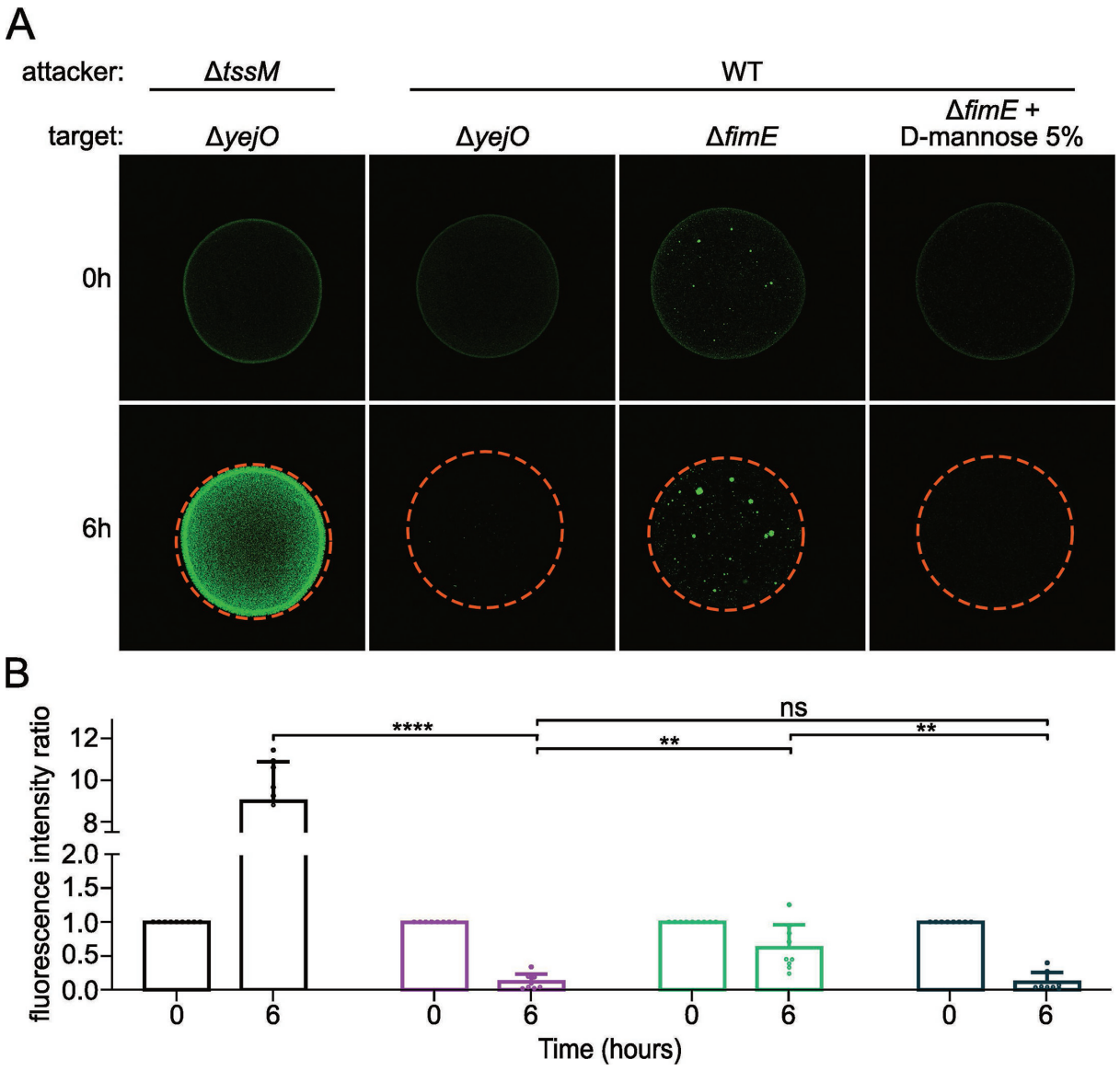

FIG 5 (A) Whole-colony microscopy reveals that type 1 fimbriae-dependent microcolonies confer resistance to the Δ*fimE* mutant against T6SS-mediated killing. Interbacterial killing was assessed using confocal microscopy and GFP-positive target cells. Attackers and targets grown overnight were mixed with a ratio of 1:1, spotted onto LB 0.8% noble agar in 12-well plates, and incubated at 37°C. The co-cultures were imaged every hour for 6 h. The colonies were delimited using orange dashed circles. (B) The killing rate was evaluated by assessing the total fluorescence inside the spot at 0 and 6 h using ImageJ and compared with the initial fluorescence rate (at 0 h). One-way ANOVA test was performed followed by Games-Howell post hoc test with Welch's correction to determine statistical significance using R (ns = nonsignificant, $^{**}P \leq 0.005$, $^{****}P \leq 0.0001$). Average ± s.d. of $n = 6–9$ replicates.

DISCUSSION

The discovery, 20 years ago, of the type 6 secretion system, a microbial weapon resembling the contractile tail of bacteriophages, changed our appreciation of bacterial dynamics within complex communities. Most studies on T6SS focus on various aspects of its biology, including biogenesis, assembly, function, and effector characterization. T6SSs inject toxic effectors directly into bacterial target cells. T6SS producers avoid autotoxicity by expressing effector-specific immunity proteins. There has been a growing interest in immunity-independent target cell defense mechanisms after the observations that envelope stress responses (26) and EPS production (29) could promote resistance to T6SS. This last study focused on the concept of spatial separation, which occurs

through the formation of microcolonies, as a strategic means to evade T6SS attacks. For example, type 4 pili, which are known to drive the formation of microcolonies (56) in *Neisseria* species, were shown to promote survival when expressed in target cells through segregation of attacker and target cells (56).

In this work, we developed a high-throughput interbacterial competition assay that allowed us to rapidly identify mutants that were resistant to T6SS-mediated killing of *C. malonaticus* 3267. *C. malonaticus* is an interesting model organism to study T6SS biology as its T6SS activity is highly effective under typical laboratory conditions (Fig. 1). The majority of gene deletions identified in our HTIC assay that conferred resistance to T6SS attacks were primarily associated with transport and metabolism (degradation and energy production), but some of our hits were previously associated with cell motility and biofilm formation, including Δ*ypdB* (57) and Δ*ymgC* (58). The product of these genes would thus impact how attacker and target cells interact together. This suggests that the modulation of the interaction dynamics between attacker and target cells could be a main strategy by which target cells can evade T6SS attacks (28, 29, 59, 60). Another hit that exhibited resistance to T6SS activity is the *ldtB* mutant. LdtB functions as a periplasmic L,D-transpeptidase which cleaves the peptide bond between *meso*-diaminopimeloyl (*m*DAP) and D-alanine in the peptidoglycan (61, 62). The T6SS-dependent activity of *C. malonaticus* is associated with the amidase effector Tae4, which is present in the T6SS cluster. The Tae4 effector is a L,D-transpeptidase that induces cell lysis by cleaving the D-Glu-*m*DAP bond in gram-negative bacteria (21). A mutant with a slightly compromised cell wall, in which the effector might potentially act, could unexpectedly exhibit resistance. Further research is required to investigate and test this concept.

We focused our analysis on the *fimE* mutant, a regulator of type 1 fimbriae production, which interestingly, appeared to confer partial protection against T6SS. Notably, the expression of type 1 fimbriae is governed by a phase variation mechanism, resulting in a heterogeneous phenotype within a clonal population. This variability could account for the observed resistance conferred by the *fimE* mutant in only two out of the three replicates. Consequently, it underscored the necessity for further investigations.

Type 1 fimbriae are rod-shaped structures found at the surface of numerous bacterial species including enteric pathogen such as enteropathogenic and enterohemorrhagic *E. coli* (63, 64). Some studies have highlighted a link between type 1 fimbriae expression and T6SS in attacker cells (65). For instance, in avian pathogenic *Escherichia coli* strains, mutations of T6SS genes decrease the expression of type 1 fimbriae, leading to lower adhesion and epithelial cells invasion (66). Our findings demonstrate that type 1 fimbriae also play a defensive role in target cells.

Our initial hypothesis was that the *fimE* mutant overexpressed type 1 fimbriae genes, resulting in their increased production. Electron microscopy and agglutination assays confirmed that the *fimE* mutant indeed increased the production of type 1 fimbriae compared to wild type (Fig. 3). The FimH adhesin, located at the tip of the type 1 fimbriae and responsible for adherence to mannose-specific receptors on host cell surfaces (67), has been previously associated with stress response behaviors, such as the internalization of fimbriated *E. coli* by macrophages in response to lethal concentrations of antibiotics (68). Moreover, adhesion appears to be an important mechanism for protection against environmental stress such as shear stress (52, 69). Adhesion mediated by type 1 fimbriae is the first step in biofilm formation (70, 71), where adherent bacteria organize themselves into microcolonies embedded within a self-produced matrix of exopolysaccharide, extracellular DNA, and proteins (72). Indeed, our whole-colony microscopy assay demonstrated that type 1 fimbriae enabled the establishment of microcolonies (Fig. 3) and that target cells within these microcolonies were protected from T6SS-mediated killing in contrast to individual bacterial cells which were efficiently killed (Fig. 5). Moreover, whole-colony microscopy of Δ*fimE* mutant in the presence of D-mannose showed that isolated fimbriated cells were killed, leading us to conclude that fimbriae alone are not sufficient to protect against T6SS attack, and emphasized that the formation of microcolonies is providing this resistance.

The synthesis of fimbriae or other adhesins such as autotransporters (73, 74), promoting the formation of microcolonies (73, 74), could represent a widespread and nonspecific defense mechanism against T6SS attacks from diverse bacteria. Accordingly, a *fim* locked-OFF strain of uropathogenic *E. coli* CFT073 still demonstrated resistance to T6SS attacks, albeit to a lesser extent than a locked-ON strain (data not shown). *E. coli* strain CFT073 possesses multiple fimbriae operons that are expressed in a coordinated manner (75). This raises questions about whether other types of fimbriae could also promote the resistance phenotype against T6SS attacks. Additionally, such structures may confer protection against various adverse stresses, including antimicrobials and reactive oxygen species. For instance, Schembri et al. demonstrated that bacterial aggregation induced by the adhesin Ag43 expression enhances survival in the presence of hydrogen peroxide (76), suggesting that the formation of microcolonies may offer broad protection against multiple stresses.

Importantly, the T6SS is not the sole contact-dependent weapon found in gram-negative bacteria. Certain contact-dependent growth inhibitions (CDI) are known to be secreted by T4SS (77) and T5SS (78). Microcolonies formed by type 1 fimbriae may therefore also provide protection to prey cells against attacker cells that use these other CDI systems. Further research is necessary to fully understand the role of type 1 fimbriae in the protection of cells under diverse stress conditions.

One of our hypotheses, supported by electron microscopy findings indicating that 50% of cells are fimbriated in the Δ*fimE* mutant, is that isolated cells constitute the nonfimbriated cell fraction of the Δ*fimE* mutant and that microcolonies were formed by the fimbriated cells. It is also possible, however, that nonfimbriated cells are also part of the microcolonies. It would therefore be interesting to identify the fimbriae-producing cells within the population in order to observe if cheaters can profit from this collective behavior. Multicellular lifestyles are prone to the presence of cheaters in the population (79). Because type 1 fimbriae are regulated through phase variation, this represents an intriguing possibility and could represent a selfless defense mechanism against the T6SS assault.

T6SS plays a crucial role in shaping microbial populations in various environments, including the gastrointestinal microbiota (34, 35, 80). Indeed, T6SS are prevalent in enteric bacteria (81). Type 1 fimbriae represent a prevalent adhesive organelle found in various members of the Enterobacteriaceae family and play a significant role as virulence factors (82). In some bacteria, those determinants act simultaneously to adhere and invade host cell (66). Studying the relationship between T6SS and type 1 fimbriae expression and, more broadly, adhesin structures in pathogenic versus host-associated bacteria *in vivo* would be an interesting line of research to elucidate the networks of genetic interactions involved in competition between bacteria.

MATERIALS AND METHODS

Strains, media, and chemicals

Bacterial strains and plasmids used in this study are listed in Table 1. Bacterial cultures were grown in Luria broth-Lennox medium (10 g/L NaCl, 5 g/L yeast extract, 5 g/L tryptone, and 15 g/L agar when needed). When required, the media were supplemented with kanamycin (50 µg/mL), ampicillin (100 µg/mL), diaminopimelic acid (0.3 mM), spectinomycin (120 µg/mL), chloramphenicol (37 µg/mL), and D-mannose 5%. Liquid cultures of *C. malonaticus* 3267 and *E. coli* BW25113 were both grown at 37°C with agitation (180 and 80 rpm, respectively).

Strain construction

Gene deletion in *C. malonaticus* 3267 was done using the lambda red recombinase system protocol (83) with minor modifications. Briefly, a spectinomycin resistance cassette was amplified from plasmid pSIM19 using primers (listed in Table 2) carrying at the 5′ end 30-nucleotide extensions homologous to regions adjacent to the gene to

be deleted. PCR products were purified, then 2 µL was transformed into *C. malonaticus* 3267 electro-competent cells carrying the red recombinase pSIM6 vector. Transformants were selected on spectinomycin plates and verified by colony PCR using primers listed in Table 2.

Growth curves

Growth was assessed using overnight culture and adjusted to an optical density (OD_{600}) of 1, diluted 1/100, and transferred to 96-well plates. The strains were grown at 37°C in a Spark 20M multimode microplate reader (TECAN), where the OD_{600} was measured every 20 min for each strain.

Particles analysis using confocal microscopy

Δ*yejO* and Δ*fimE* prey strains were cultured in liquid overnight and were next adjusted to an OD_{600} of 1. Then, 5% D-mannose was added to Δ*fimE* prey culture when required, and 2 µL was spotted onto LB 0.8% noble agar in 12-well plates in duplicate. The particles were observed using a 20× magnification FV3000 Olympus confocal microscope for three independent experiments. For each experiment, strains were spotted in duplicate. Three images were taken at random coordinates for each duplicate. Particle sizes were assessed using the ImageJ "Analyze Particles" function.

Interbacterial competition assay

C. malonaticus 3267 WT and Δ*tssM* mutants were used as attacker cells. *E. coli* BW25113 Δ*fimE* and Δ*yejO* were used as target cells for interbacterial competition assay. Attackers and targets were grown in liquid media overnight. The cultures were adjusted to an OD_{600} of 1. And, 5% D-mannose was added to target cultures when required. Approximately 10^7 bacteria were combined at a ratio of 1:1, then 5 µL was spotted onto sterile nitrocellulose filters on LB agar plate and incubated for 24 h at 37°C. The co-cultures were resuspended in 1 mL of LB broth. Serial dilutions were plated onto LB selective medium to assess the number of CFUs of surviving target cells. The experiment was repeated three times independently. For the complementation assay, *E. coli* BW25113 Δ*yejO* pCA24N, Δ*fimE* pCA24N, and Δ*fimE* pCA24N-*fimE* were used as targets, and the expression of genes from pCA24N vector was induced with 10 µM of isopropyl-β-D-thiogalactopyranoside in overnight liquid cultures and competition agar plates used for interbacterial competition.

High-throughput interbacterial competition assay

Attackers *C. malonaticus* 3267 WT and Δ*tssM* mutants were grown in overnight liquid cultures at 37°C. Next day, the cultures were pinned on agar plates with 1,536-pin pad

TABLE 1 Bacterial strains and plasmids used in this study

Strain or plasmid	Description	Source
Cronobacter malonaticus 3267	Wild type	This study
Δ*tssM::aadA(smR)*	*tssM* gene deletion mutant from *Cronobacter malonaticus* 3267	This study
Keio collection	Mutant collection of all nonessential genes from *E. coli* K-12 BW25113. F−, Δ(*araD-araB*)567, λ−, rph-1, Δ(*rhaD-rhaB*)568, *hsdR*514	KEIO collection (40)
Δ*yejO::nptII(kanR)*	*yejO* pseudo gene deletion mutant from *E. coli* K-12 BW25113. Considered as *WT*	This study
Δ*fimE::nptII(kanR)*	*fimE* gene deletion mutant from *E. coli* K-12 BW25113	This study
pCA24N	Cm^R, IPTG-inducible promotor	ASKA collection (43)
pCA24N-*fimE*	Cm^R, IPTG-inducible promotor, expression of FimE	ASKA collection (43)
pKD3	Template plasmids for frt-flanked cat cassette. cat cassette originally came from pSC140	(83)
pSIM19	Sm^R, pSC101 $repA^{ts}$	(84)
pSIM6	Amp^R, pSC101 $repA^{ts}$	(85)
pTrcGFP	Amp^R, green fluorescent protein expression, pTrc99a backbone	This study

TABLE 2 Primers used in this study

Primer type and gene	F/R	Sequence
Gene deletion		
tssM	F	taaagcgctgcaaaccaccgccgggcgcgatctcttcagcgtgtaggctggagctgcttc
tssM	R	gctaatcgcagggtaatgactcattatccgttccttgcggcatatgaatatcctccttag
Colony PCR verification		
tssM	F1	acgtgattttccaggaagcgg
tssM	F2	ccacggaatgatgtcgtcg
tssM	R1	ggagtgaataccacgacgat
tssM	R1	cgacgacatcattccgtgg

using the Rotor HDA (Singer Instruments, United Kingdom), then incubated 1 h at 37°C. The Keio collection was grown, in parallel, for 2 h in 384-well plates at 37°C, directly from 384-well plates stored at −80°C. Keio mutants were then pinned onto competition agar plates and incubated for 24 h at 37°C. Survival was assessed by pinning onto kanamycin selection plates. Surviving was assessed for each replicate using binary value; any growth refers to resistance (=1), no growth means that the mutant is sensitive (=0). In this experiment, a mutant was considered resistant if there was growth in at least two of the three replicates.

Yeast agglutination assay

Strains used in this assay were grown overnight in liquid media. The cultures were adjusted to an OD_{600} of 6 and then centrifuged at 5,000 rpm for 5 min and then resuspended in 5 mL of phosphate buffered saline (PBS, pH 7.2). Yeast cells were resuspended in 5 mL of PBS. And, 5% D-mannose was added when required. Cells were mixed at a ratio of 1:1, then 20 µL was spotted onto glass slides.

Electron microscopy

Twenty-four-hour colonies grown on agar plates at 37°C for 24 h were resuspended in HEPES buffer and then deposited on carbon-supported grids at room temperature. Samples were negatively stained with 2% of uranyl acetate. Negatively stained bacterial cells were examined with a TECNAI G2 electron microscope. Fifty pictures were acquired for each condition. All bacteria were considered for counting the number of fimbriae per cell.

Interbacterial competition assay in macrocolony and observation using confocal microscopy

Interbacterial competition assays were performed as described by Granato et al. (29) with minor modifications. Briefly, target cells carrying the pTrcGFP strong gfp-expressing vector were grown in liquid media overnight with 100 µg/mL of ampicillin. The cultures were adjusted to an OD_{600} of 1. D-mannose (5%) was added when required. Approximately 10^6 bacteria were combined at a ratio of 1:1, then 2 µL was spotted on LB 0.8% noble agar in 12-well plates and incubated at 37°C, and images were acquired every hour for 6 h using a 20× magnification FV3000 Olympus confocal microscope. The killing rate was evaluated by assessing the total fluorescence inside the spot at 0 and 6 h using ImageJ.

Statistical analysis

All experiments were carried out at least three times with at least two biological replicates for each experiment except for the electron microscopy assay. Statistical analyses were made using R. The normal distribution of the data was first assessed, followed by a Levene's test to examine the homogeneity of standard deviations across samples. The choice of whether to use parametric or nonparametric tests to analyze

the data was made in accordance with the results obtained for the normality tests. The choice between ANOVA and two-group comparison tests depended on the number of groups under analysis.

ACKNOWLEDGMENTS

We thank Daphnée Lamarche for insightful comments on the manuscript.

This work was supported by the Natural Science and Engineering Research Council of Canada (RGPIN-2019-06044). J.-P.C. holds a Chercheur boursier junior 1 fellowship from the Fonds de recherche du Québec-Santé (FRQS).

AUTHOR AFFILIATIONS

[1]Département de biologie, Faculté des sciences, Université de Sherbrooke, Sherbrooke, Quebec, Canada
[2]Plateforme de microscopie, Institut de Microbiologie de la Méditerranée (IMM, FR3479), Aix-Marseille Univ, CNRS, Marseille, France
[3]Laboratoire d'Ingénierie des Systèmes Macromoléculaires (LISM, UMR7255), Institut de Microbiologie de la Méditerranée, Aix Marseille Univ, CNRS, Marseille, France

AUTHOR ORCIDs

Margot Marie Dessartine http://orcid.org/0009-0005-8798-8537
Éric Cascales http://orcid.org/0000-0003-0611-9179
Jean-Philippe Côté http://orcid.org/0000-0003-3971-6834

FUNDING

Funder	Grant(s)	Author(s)
Canadian Government | Natural Sciences and Engineering Research Council of Canada (NSERC)	RGPIN-2019-06044	Jean-Philippe Côté
FRQ | Fonds de Recherche du Québec - Santé (FRQS)	281803	Jean-Philippe Côté

AUTHOR CONTRIBUTIONS

Margot Marie Dessartine, Conceptualization, Formal analysis, Investigation, Methodology, Writing – original draft | Artemis Kosta, Investigation, Methodology | Thierry Doan, Investigation, Methodology | Éric Cascales, Conceptualization, Funding acquisition, Resources, Supervision, Writing – review and editing | Jean-Philippe Côté, Conceptualization, Funding acquisition, Project administration, Resources, Supervision, Writing – review and editing

ADDITIONAL FILES

The following material is available online.

Supplemental Material

Supplemental material (mBio02553-23-s0001.docx). Supplemental figures and tables.

REFERENCES

1. Hibbing ME, Fuqua C, Parsek MR, Peterson SB. 2010. Bacterial competition: surviving and thriving in the microbial jungle. Nat Rev Microbiol 8:15–25. https://doi.org/10.1038/nrmicro2259
2. Künzler M. 2018. How fungi defend themselves against microbial competitors and animal predators. PLoS Pathog 14:e1007184. https://doi.org/10.1371/journal.ppat.1007184
3. Bao H, Wang S, Zhao JH, Liu SL. 2020. *Salmonella* secretion systems: differential roles in pathogen-host interactions. Microbiol Res 241:126591. https://doi.org/10.1016/j.micres.2020.126591
4. Waksman G. 2012. Bacterial secretion comes of age. Philos Trans R Soc Lond B Biol Sci 367:1014–1015. https://doi.org/10.1098/rstb.2011.0200

5. Si M, Wang Y, Zhang B, Zhao C, Kang Y, Bai H, Wei D, Zhu L, Zhang L, Dong TG, Shen X. 2017. The type VI secretion system engages a redox-regulated dual-functional heme transporter for zinc acquisition. Cell Rep 20:949–959. https://doi.org/10.1016/j.celrep.2017.06.081
6. Wan B, Zhang Q, Ni J, Li S, Wen D, Li J, Xiao H, He P, Ou H-Y, Tao J, Teng Q, Lu J, Wu W, Yao Y-F. 2017. Type VI secretion system contributes to Enterohemorrhagic *Escherichia coli* virulence by secreting catalase against host reactive oxygen species (ROS). PLoS Pathog 13:e1006246. https://doi.org/10.1371/journal.ppat.1006246
7. Mougous JD, Cuff ME, Raunser S, Shen A, Zhou M, Gifford CA, Goodman AL, Joachimiak G, Ordoñez CL, Lory S, Walz T, Joachimiak A, Mekalanos JJ. 2006. A virulence locus of *Pseudomonas aeruginosa* encodes a protein secretion apparatus. Science 312:1526–1530. https://doi.org/10.1126/science.1128393
8. Pukatzki S, Ma AT, Sturtevant D, Krastins B, Sarracino D, Nelson WC, Heidelberg JF, Mekalanos JJ. 2006. Identification of a conserved bacterial protein secretion system in *Vibrio cholerae* using the *Dictyostelium* host model system. Proc Natl Acad Sci U S A 103:1528–1533. https://doi.org/10.1073/pnas.0510322103
9. Chassaing B, Cascales E. 2018. Antibacterial weapons: targeted destruction in the microbiota. Trends Microbiol 26:329–338. https://doi.org/10.1016/j.tim.2018.01.006
10. Chatzidaki-Livanis M, Geva-Zatorsky N, Comstock LE. 2016. *Bacteroides fragilis* type VI secretion systems use novel effector and immunity proteins to antagonize human gut Bacteroidales species. Proc Natl Acad Sci U S A 113:3627–3632. https://doi.org/10.1073/pnas.1522510113
11. Sana TG, Flaugnatti N, Lugo KA, Lam LH, Jacobson A, Baylot V, Durand E, Journet L, Cascales E, Monack DM. 2016. *Salmonella* Typhimurium utilizes a T6SS-mediated antibacterial weapon to establish in the host gut. Proc Natl Acad Sci U S A 113:E5044–E5051. https://doi.org/10.1073/pnas.1608858113
12. Cianfanelli FR, Monlezun L, Coulthurst SJ. 2016. Aim, load, fire: the type VI secretion system, a bacterial nanoweapon. Trends Microbiol 24:51–62. https://doi.org/10.1016/j.tim.2015.10.005
13. Yang X, Long M, Shen X. 2018. Effector–immunity pairs provide the T6SS nanomachine its offensive and defensive capabilities. Molecules 23:1009. https://doi.org/10.3390/molecules23051009
14. Brunet YR, Zoued A, Boyer F, Douzi B, Cascales E. 2015. The type VI secretion TssEFGK-VgrG phage-like baseplate is recruited to the TssJLM membrane complex via multiple contacts and serves as assembly platform for tail tube/sheath polymerization. PLoS Genet 11:e1005545. https://doi.org/10.1371/journal.pgen.1005545
15. Durand E, Nguyen VS, Zoued A, Logger L, Péhau-Arnaudet G, Aschtgen MS, Spinelli S, Desmyter A, Bardiaux B, Dujeancourt A, Roussel A, Cambillau C, Cascales E, Fronzes R. 2015. Biogenesis and structure of a type VI secretion membrane core complex. Nature 523:555–560. https://doi.org/10.1038/nature14667
16. Zoued A, Brunet YR, Durand E, Aschtgen MS, Logger L, Douzi B, Journet L, Cambillau C, Cascales E. 2014. Architecture and assembly of the type VI secretion system. Biochim Biophys Acta 1843:1664–1673. https://doi.org/10.1016/j.bbamcr.2014.03.018
17. Ballister ER, Lai AH, Zuckermann RN, Cheng Y, Mougous JD. 2008. *In vitro* self-assembly of tailorable nanotubes from a simple protein building block. Proc Natl Acad Sci U S A 105:3733–3738. https://doi.org/10.1073/pnas.0712247105
18. Lossi NS, Manoli E, Förster A, Dajani R, Pape T, Freemont P, Filloux A. 2013. The HsiB1C1 (TssB-TssC) complex of the *Pseudomonas aeruginosa* type VI secretion system forms a bacteriophage tail Sheathlike structure. J Biol Chem 288:7536–7548. https://doi.org/10.1074/jbc.M112.439273
19. Shneider MM, Buth SA, Ho BT, Basler M, Mekalanos JJ, Leiman PG. 2013. PAAR-repeat proteins sharpen and diversify the type VI secretion system spike. Nature 500:350–353. https://doi.org/10.1038/nature12453
20. Russell AB, LeRoux M, Hathazi K, Agnello DM, Ishikawa T, Wiggins PA, Wai SN, Mougous JD. 2013. Diverse type VI secretion phospholipases are functionally plastic antibacterial effectors. Nature 496:508–512. https://doi.org/10.1038/nature12074
21. Benz J, Reinstein J, Meinhart A. 2013. Structural insights into the effector – immunity system Tae4/Tai4 from *Salmonella* typhimurium. PLoS One 8:e67362. https://doi.org/10.1371/journal.pone.0067362
22. Ma LS, Hachani A, Lin JS, Filloux A, Lai EM. 2014. *Agrobacterium tumefaciens* deploys a superfamily of type VI secretion DNase effectors as weapons for interbacterial competition in planta. Cell Host Microbe 16:94–104. https://doi.org/10.1016/j.chom.2014.06.002
23. Coulthurst S. 2019. The type VI secretion system: a versatile bacterial weapon. Microbiology (Reading) 165:503–515. https://doi.org/10.1099/mic.0.000789
24. Bai Q, Ma J, Zhang Z, Zhong X, Pan Z, Zhu Y, Zhang Y, Wu Z, Liu G, Yao H. 2020. YSIRK-G/S-directed translocation is required for *Streptococcus suis* to deliver diverse cell wall anchoring effectors contributing to bacterial pathogenicity. Virulence 11:1539–1556. https://doi.org/10.1080/21505594.2020.1838740
25. Whitney JC, Beck CM, Goo YA, Russell AB, Harding BN, De Leon JA, Cunningham DA, Tran BQ, Low DA, Goodlett DR, Hayes CS, Mougous JD. 2014. Genetically distinct pathways guide effector export through the type VI secretion system. Mol Microbiol 92:529–542. https://doi.org/10.1111/mmi.12571
26. Hersch SJ, Watanabe N, Stietz MS, Manera K, Kamal F, Burkinshaw B, Lam L, Pun A, Li M, Savchenko A, Dong TG. 2020. Envelope stress responses defend against type six secretion system attacks independently of immunity proteins. Nat Microbiol 5:706–714. https://doi.org/10.1038/s41564-020-0672-6
27. Hersch SJ, Manera K, Dong TG. 2020. Defending against the type six secretion system: beyond immunity genes. Cell Rep 33:108259. https://doi.org/10.1016/j.celrep.2020.108259
28. Borenstein DB, Ringel P, Basler M, Wingreen NS. 2015. Established microbial colonies can survive type VI secretion assault. PLoS Comput Biol 11:e1004520. https://doi.org/10.1371/journal.pcbi.1004520
29. Granato ET, Smith WPJ, Foster KR. 2023. Collective protection against the type VI secretion system in bacteria. ISME J 17:1052–1062. https://doi.org/10.1038/s41396-023-01401-4
30. Lories B, Roberfroid S, Dieltjens L, De Coster D, Foster KR, Steenackers HP. 2020. Biofilm bacteria use stress responses to detect and respond to competitors. Curr Biol 30:1231–1244. https://doi.org/10.1016/j.cub.2020.01.065
31. Smith WPJ, Vettiger A, Winter J, Ryser T, Comstock LE, Basler M, Foster KR. 2020. The evolution of the type VI secretion system as a disintegration weapon. PLoS Biol 18:e3000720. https://doi.org/10.1371/journal.pbio.3000720
32. Nwoko E-SQA, Okeke IN. 2021. Bacteria autoaggregation: how and why bacteria stick together. Biochem Soc Trans 49:1147–1157. https://doi.org/10.1042/BST20200718
33. Lang C, Fruth A, Holland G, Laue M, Mühlen S, Dersch P, Flieger A. 2018. Novel type of pilus associated with a Shiga-toxigenic *E. coli* hybrid pathovar conveys aggregative adherence and bacterial virulence. Emerg Microbes Infect 7:203. https://doi.org/10.1038/s41426-018-0209-8
34. Allsopp LP, Bernal P, Nolan LM, Filloux A. 2020. Causalities of war: the connection between type VI secretion system and microbiota. Cell Microbiol 22:e13153. https://doi.org/10.1111/cmi.13153
35. Zhao W, Caro F, Robins W, Mekalanos JJ. 2018. Antagonism toward the intestinal microbiota and its effect on *Vibrio cholerae* virulence. Science 359:210–213. https://doi.org/10.1126/science.aap8775
36. Paradis-Bleau C, Kritikos G, Orlova K, Typas A, Bernhardt TG. 2014. A genome-wide screen for bacterial envelope biogenesis mutants identifies a novel factor involved in cell wall precursor metabolism. PLoS Genet 10:e1004056. https://doi.org/10.1371/journal.pgen.1004056
37. Côté J-P, French S, Gehrke SS, MacNair CR, Mangat CS, Bharat A, Brown ED. 2016. The genome-wide interaction network of nutrient stress genes in *Escherichia coli*. mBio 7:e01714-16. https://doi.org/10.1128/mBio.01714-16
38. Ben-Yaakov R, Salomon D. 2019. The regulatory network of *Vibrio parahaemolyticus* type VI secretion system 1. Environ Microbiol 21:2248–2260. https://doi.org/10.1111/1462-2920.14594
39. Healy B, Cooney S, O'Brien S, Iversen C, Whyte P, Nally J, Callanan JJ, Fanning S. 2010. *Cronobacter* (*Enterobacter sakazakii*): an opportunistic foodborne pathogen. Foodborne Pathog Dis 7:339–350. https://doi.org/10.1089/fpd.2009.0379
40. Baba T, Ara T, Hasegawa M, Takai Y, Okumura Y, Baba M, Datsenko KA, Tomita M, Wanner BL, Mori H. 2006. Construction of *Escherichia coli* K-12 in-frame, single-gene knockout mutants: the Keio collection. Mol Syst Biol 2:2006. https://doi.org/10.1038/msb4100050

41. Wang M, Cao H, Wang Q, Xu T, Guo X, Liu B. 2018. The roles of two type VI secretion systems in *Cronobacter sakazakii* ATCC 12868. Front Microbiol 9:2499. https://doi.org/10.3389/fmicb.2018.02499
42. Hasman H, Schembri MA, Klemm P. 2000. Antigen 43 and type 1 fimbriae determine colony morphology of *Escherichia coli* K-12. J Bacteriol 182:1089–1095. https://doi.org/10.1128/JB.182.4.1089-1095.2000
43. Kitagawa M, Ara T, Arifuzzaman M, Ioka-Nakamichi T, Inamoto E, Toyonaga H, Mori H. 2005. Complete set of ORF clones of *Escherichia coli* ASKA library (A complete set of *E. coli* K-12 ORF archive): unique resources for biological research. DNA Res 12:291–299. https://doi.org/10.1093/dnares/dsi012
44. Soto GE, Hultgren SJ. 1999. Bacterial adhesins: common themes and variations in architecture and assembly. J Bacteriol 181:1059–1071. https://doi.org/10.1128/JB.181.4.1059-1071.1999
45. Eisenstein BI. 1981. Phase variation of type 1 fimbriae in *Escherichia coli* is under transcriptional control. Science 214:337–339. https://doi.org/10.1126/science.6116279
46. Klemm P. 1986. Two regulatory *fim* genes, *fimB* and *fimE*, control the phase variation of type 1 fimbriae in *Escherichia coli*. EMBO J 5:1389–1393. https://doi.org/10.1002/j.1460-2075.1986.tb04372.x
47. Gally DL, Leathart J, Blomfield IC. 1996. Interaction of FimB and FimE with the fim switch that controls the phase variation of type 1 fimbriae in *Escherichia coli* K-12. Mol Microbiol 21:725–738. https://doi.org/10.1046/j.1365-2958.1996.311388.x
48. Bessaiah H, Anamalé C, Sung J, Dozois CM. 2021. What flips the switch? Signals and stress regulating extraintestinal pathogenic *Escherichia coli* type 1 fimbriae (pili). Microorganisms 10:5. https://doi.org/10.3390/microorganisms10010005
49. Dorman CJ, Higgins CF. 1987. Fimbrial phase variation in *Escherichia coli*: dependence on integration host factor and homologies with other site-specific recombinases. J Bacteriol 169:3840–3843. https://doi.org/10.1128/jb.169.8.3840-3843.1987
50. Orndorff PE, Falkow S. 1984. Identification and characterization of a gene product that regulates type 1 piliation in *Escherichia coli*. J Bacteriol 160:61–66. https://doi.org/10.1128/jb.160.1.61-66.1984
51. Blomfield IC, McClain MS, Princ JA, Calie PJ, Eisenstein BI. 1991. Type 1 fimbriation and *fimE* mutants of *Escherichia coli* K-12. J Bacteriol 173:5298–5307. https://doi.org/10.1128/jb.173.17.5298-5307.1991
52. Thomas WE, Nilsson LM, Forero M, Sokurenko EV, Vogel V. 2004. Shear-dependent "stick-and-roll" adhesion of type 1 fimbriated *Escherichia coli*. Mol Microbiol 53:1545–1557. https://doi.org/10.1111/j.1365-2958.2004.04226.x
53. Brinton CC. 1965. The structure, function, synthesis and genetic control of bacterial pili and a molecular model for DNA and RNA transport in Gram negative bacteria. Trans NY Acad Sci 27:1003–1054. https://doi.org/10.1111/j.2164-0947.1965.tb02342.x
54. Krogfelt KA, Bergmans H, Klemm P. 1990. Direct evidence that the FimH protein is the mannose-specific adhesion of *Escherichia coli* type 1 fimbriae. Infect Immun 58:1995–1998. https://doi.org/10.1128/iai.58.6.1995-1998.1990
55. Ofek I, Mirelman D, Sharon N. 1977. Adherence of *Escherichia coli* to human mucosal cells mediated by mannose receptors. Nature 265:623–625. https://doi.org/10.1038/265623a0
56. Higashi DL, Lee SW, Snyder A, Weyand NJ, Bakke A, So M. 2007. Dynamics of *Neisseria gonorrhoeae* attachment: microcolony development, cortical plaque formation, and cytoprotection. Infect Immun 75:4743–4753. https://doi.org/10.1128/IAI.00687-07
57. Kim K, Lee S, Ryu C-M. 2013. Interspecific bacterial sensing through airborne signals modulates locomotion and drug resistance. Nat Commun 4:1809. https://doi.org/10.1038/ncomms2789
58. Lee J, Page R, García-Contreras R, Palermino J-M, Zhang X-S, Doshi O, Wood TK, Peti W. 2007. Structure and function of the *Escherichia coli* protein YmgB: a protein critical for biofilm formation and acid-resistance. J Mol Biol 373:11–26. https://doi.org/10.1016/j.jmb.2007.07.037
59. Rudzite M, Subramoni S, Endres RG, Filloux A. 2023. Effectiveness of *Pseudomonas aeruginosa* type VI secretion system relies on toxin potency and type IV pili-dependent interaction. PLoS Pathog 19:e1011428. https://doi.org/10.1371/journal.ppat.1011428
60. Lin L, Capozzoli R, Ferrand A, Plum M, Vettiger A, Basler M. 2022. Subcellular localization of type VI secretion system assembly in response to cell–cell contact. EMBO J 41:e108595. https://doi.org/10.15252/embj.2021108595
61. Magnet S, Bellais S, Dubost L, Fourgeaud M, Mainardi J-L, Petit-Frère S, Marie A, Mengin-Lecreulx D, Arthur M, Gutmann L. 2007. Identification of the L,D-transpeptidases responsible for attachment of the Braun lipoprotein to *Escherichia coli* peptidoglycan. J Bacteriol 189:3927–3931. https://doi.org/10.1128/JB.00084-07
62. Braun V, Wolff H. 1970. The murein-lipoprotein linkage in the cell wall of *Escherichia coli*. Eur J Biochem 14:387–391. https://doi.org/10.1111/j.1432-1033.1970.tb00301.x
63. Kaper JB, Nataro JP, Mobley HLT. 2004. Pathogenic *Escherichia coli*. Nat Rev Microbiol 2:123–140. https://doi.org/10.1038/nrmicro818
64. Hannan TJ, Totsika M, Mansfield KJ, Moore KH, Schembri MA, Hultgren SJ, Stoever HL. 2012. Host-pathogen checkpoints and population bottlenecks in persistent and intracellular uropathogenic *E. coli* bladder infection. FEMS Microbiol Rev 36:616–648. https://doi.org/10.1111/j.1574-6976.2012.00339.x
65. Hsieh P-F, Lu Y-R, Lin T-L, Lai L-Y, Wang J-T. 2019. *Klebsiella pneumoniae* type VI secretion system contributes to bacterial competition, cell invasion, type-1 fimbriae expression, and *in vivo* colonization. J Infect Dis 219:637–647. https://doi.org/10.1093/infdis/jiy534
66. de Pace F, Nakazato G, Pacheco A, de Paiva JB, Sperandio V, da Silveira WD. 2010. The type VI secretion system plays a role in type 1 fimbria expression and pathogenesis of an avian pathogenic *Escherichia coli* strain. Infect Immun 78:4990–4998. https://doi.org/10.1128/IAI.00531-10
67. Duan Q, Nandre R, Zhou M, Zhu G. 2017. Type I fimbriae mediate *in vitro* adherence of porcine F18ac+ enterotoxigenic *Escherichia coli* (ETEC). Ann Microbiol 67:793–799. https://doi.org/10.1007/s13213-017-1305-z
68. Avalos Vizcarra I, Hosseini V, Kollmannsberger P, Meier S, Weber SS, Arnoldini M, Ackermann M, Vogel V. 2016. How type 1 fimbriae help *Escherichia coli* to evade extracellular antibiotics. Sci Rep 6:18109. https://doi.org/10.1038/srep18109
69. Wang L, Keatch R, Zhao Q, Wright JA, Bryant CE, Redmann AL, Terentjev EM. 2018. Influence of type I fimbriae and fluid shear stress on bacterial behavior and multicellular architecture of early *Escherichia coli* biofilms at single-cell resolution. Appl Environ Microbiol 84:e02343-17. https://doi.org/10.1128/AEM.02343-17
70. Lasaro MA, Salinger N, Zhang J, Wang Y, Zhong Z, Goulian M, Zhu J. 2009. F1C fimbriae play an important role in biofilm formation and intestinal colonization by the *Escherichia coli* commensal strain Nissle 1917. Appl Environ Microbiol 75:246–251. https://doi.org/10.1128/AEM.01144-08
71. Liu Q, Zhu J, Liu N, Sun W, Yu B, Niu H, Liu D, Ouyang P, Ying H, Chen Y, Zhao G, Chen T. 2022. Type I fimbriae subunit *fimA* enhances *Escherichia coli* biofilm formation but affects L-threonine carbon distribution. Front Bioeng Biotechnol 10:904636. https://doi.org/10.3389/fbioe.2022.904636
72. Penesyan A, Paulsen IT, Kjelleberg S, Gillings MR. 2021. Three faces of biofilms: a microbial lifestyle, a nascent multicellular organism, and an incubator for diversity. NPJ Biofilms Microbiomes 7:80. https://doi.org/10.1038/s41522-021-00251-2
73. Sherlock O, Vejborg RM, Klemm P. 2005. The TibA adhesin/invasin from enterotoxigenic *Escherichia coli* is self recognizing and induces bacterial aggregation and biofilm formation. Infect Immun 73:1954–1963. https://doi.org/10.1128/IAI.73.4.1954-1963.2005
74. Côté J-P, Mourez M. 2011. Structure-function analysis of the TibA self-associating autotransporter reveals a modular organization. Infect Immun 79:1826–1832. https://doi.org/10.1128/IAI.01129-10
75. Snyder JA, Haugen BJ, Lockatell CV, Maroncle N, Hagan EC, Johnson DE, Welch RA, Mobley HLT. 2005. Coordinate expression of fimbriae in uropathogenic *Escherichia coli*. Infect Immun 73:7588–7596. https://doi.org/10.1128/IAI.73.11.7588-7596.2005
76. Schembri MA, Hjerrild L, Gjermansen M, Klemm P. 2003. Differential expression of the *Escherichia coli* autoaggregation factor antigen 43. J Bacteriol 185:2236–2242. https://doi.org/10.1128/JB.185.7.2236-2242.2003
77. Souza DP, Oka GU, Alvarez-Martinez CE, Bisson-Filho AW, Dunger G, Hobeika L, Cavalcante NS, Alegria MC, Barbosa LRS, Salinas RK, Guzzo CR,

Farah CS. 2015. Bacterial killing via a type IV secretion system. Nat Commun 6:6453. https://doi.org/10.1038/ncomms7453
78. Aoki SK, Pamma R, Hernday AD, Bickham JE, Braaten BA, Low DA. 2005. Contact-dependent inhibition of growth in *Escherichia coli*. Science 309:1245–1248. https://doi.org/10.1126/science.1115109
79. Smith P, Schuster M. 2019. Public goods and cheating in microbes. Curr Biol 29:R442–R447. https://doi.org/10.1016/j.cub.2019.03.001
80. Chen C, Yang X, Shen X. 2019. Confirmed and potential roles of bacterial T6SSs in the intestinal ecosystem. Front Microbiol 10:1484. https://doi.org/10.3389/fmicb.2019.01484
81. Coyne MJ, Comstock LE. 2019. Type VI secretion systems and the gut microbiota. Microbiol Spectr 7. https://doi.org/10.1128/microbiolspec.PSIB-0009-2018
82. Pakbin B, Brück WM, Rossen JWA. 2021. Virulence factors of enteric pathogenic *Escherichia coli*: a review. Int J Mol Sci 22:9922. https://doi.org/10.3390/ijms22189922
83. Datsenko KA, Wanner BL. 2000. One-step inactivation of chromosomal genes in *Escherichia coli* K-12 using PCR products. Proc Natl Acad Sci U S A 97:6640–6645. https://doi.org/10.1073/pnas.120163297
84. Sharan SK, Thomason LC, Kuznetsov SG, Court DL. 2009. Recombineering: a homologous recombination-based method of genetic engineering. Nat Protoc 4:206–223. https://doi.org/10.1038/nprot.2008.227
85. Datta S, Costantino N, Court DL. 2006. A set of recombineering plasmids for gram-negative bacteria. Gene 379:109–115. https://doi.org/10.1016/j.gene.2006.04.018

Supplemental Materials

Type 1 fimbriae-mediated collective protection against type 6 secretion system attacks

Margot Marie Dessartine[1], Artemis Kosta[3], Thierry Doan[2], Éric Cascales[2], Jean-Philippe Côté[1#]

[1] Département de biologie, Faculté des sciences, Université de Sherbrooke, Sherbrooke, QC J1K 2R1, Canada.

[2] Laboratoire d'Ingénierie des Systèmes Macromoléculaires (LISM, UMR7255), Institut de Microbiologie de la Méditerranée, Aix Marseille Univ, CNRS, Marseille, France

[3] Plateforme de microscopie, Institut de Microbiologie de la Méditerranée (IMM, FR3479), Aix-Marseille Univ, CNRS, Marseille, France

Correspondence may be addressed to:

Jean-Philippe Côté
Tel :1-819-821-8000 ext. 65280
Email: jp.cote@usherbrooke.ca

This Supplemental Material includes:

Supplementary Figures 1 to 4

Supplementary Tables 1 and 2

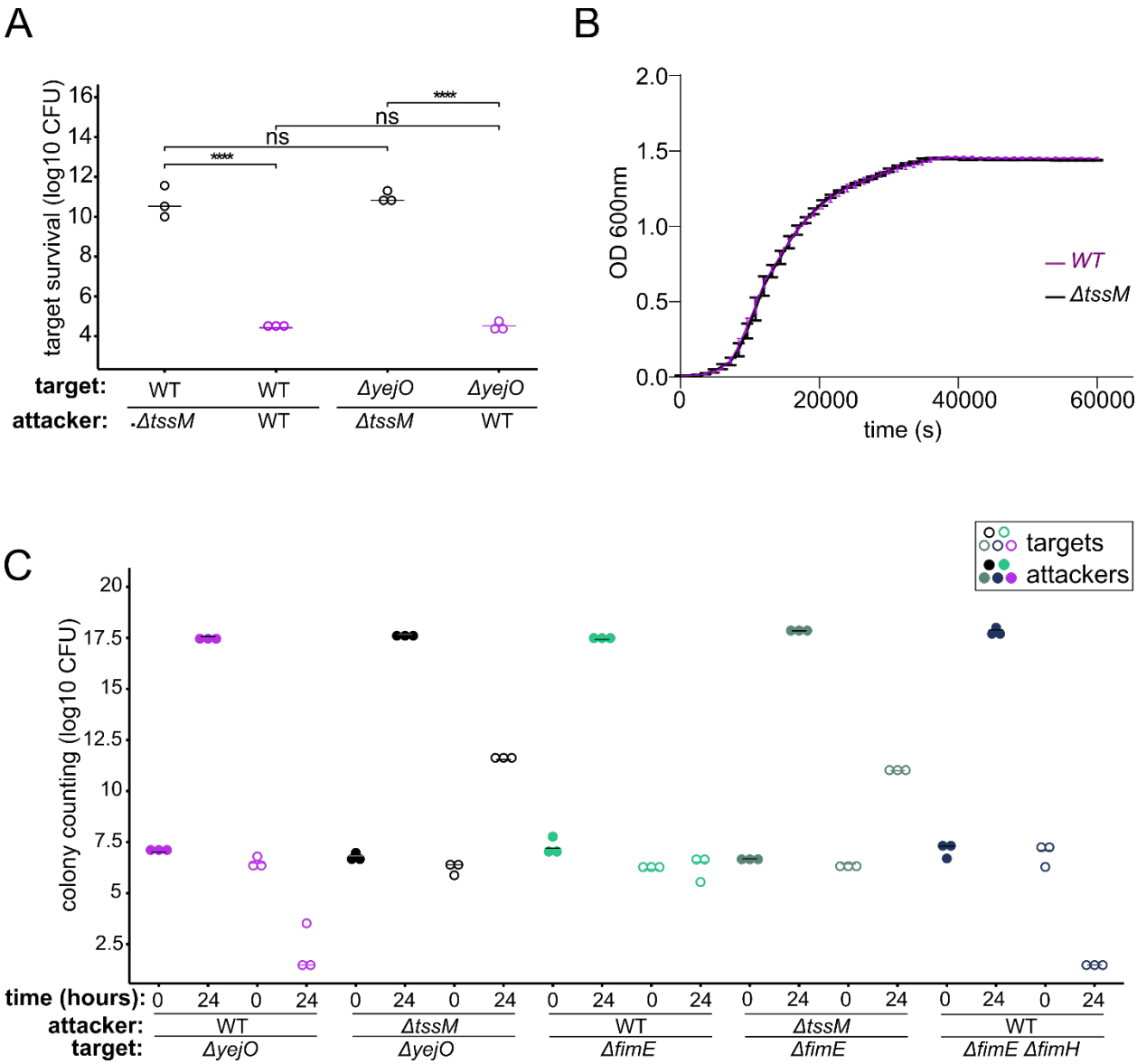

Supplementary Fig. 1: (A) Interbacterial competition assay between *C. malonaticus* 3267 WT or Δ*tssM* attackers and Δ*yejO* and BW25113 WT target cells. Target survival is presented in Log10 CFU. One-way Anova test was used followed by Tukey post-hoc test to determine statistical significance (ns=nonsignificant, ****p≤0.0001). Data represent three independent experiments (B) Growth curves of *C. malonaticus* 3267 WT and Δ*tssM* is shown. Overnight cultures of attacker strains were diluted 100 times, transferred to 96-well plates, and grown for 17 hours. OD_{600} was measured every 20 min for each strain. The data represent the mean (±SD) of three independent experiments. (C) Interbacterial competition assay between WT or Δ*tssM* attackers and *E. coli* Δ*yejO*, Δ*fimE* and Δ*fimEH* target cells. Attacker and target survival is assessed at 0h and 24h after an interbacterial competition assay and is presented in Log10 CFU. Filled circles represent attackers and empty circles represent targets.

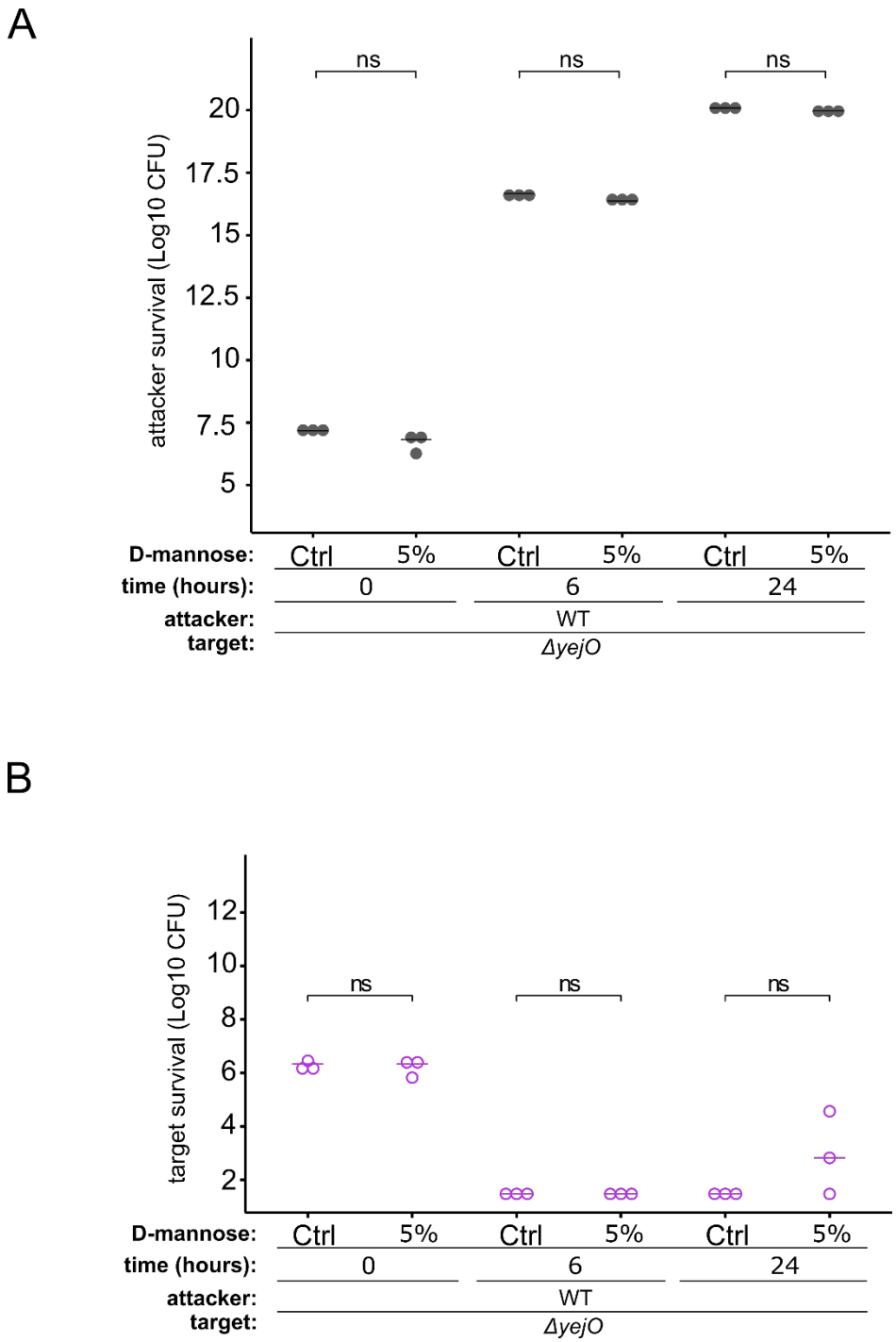

Supplementary Fig. 2: Interbacterial competition assay between C. malonaticus *3267* WT attacker and Δ*yejO* target cells (with and without 5% of D-mannose). (A) Attacker survival at 0h, 6h and 24h following interbacterial killing assay is presented in Log10 CFU. (B) Target survival at 0h, 6h and 24h following interbacterial killing assay is presented in Log10 CFU. One-way Anova test was used followed by Tukey post-hoc test to determine statistical significance using R (ns=nonsignificant). Data represent three independent experiments.

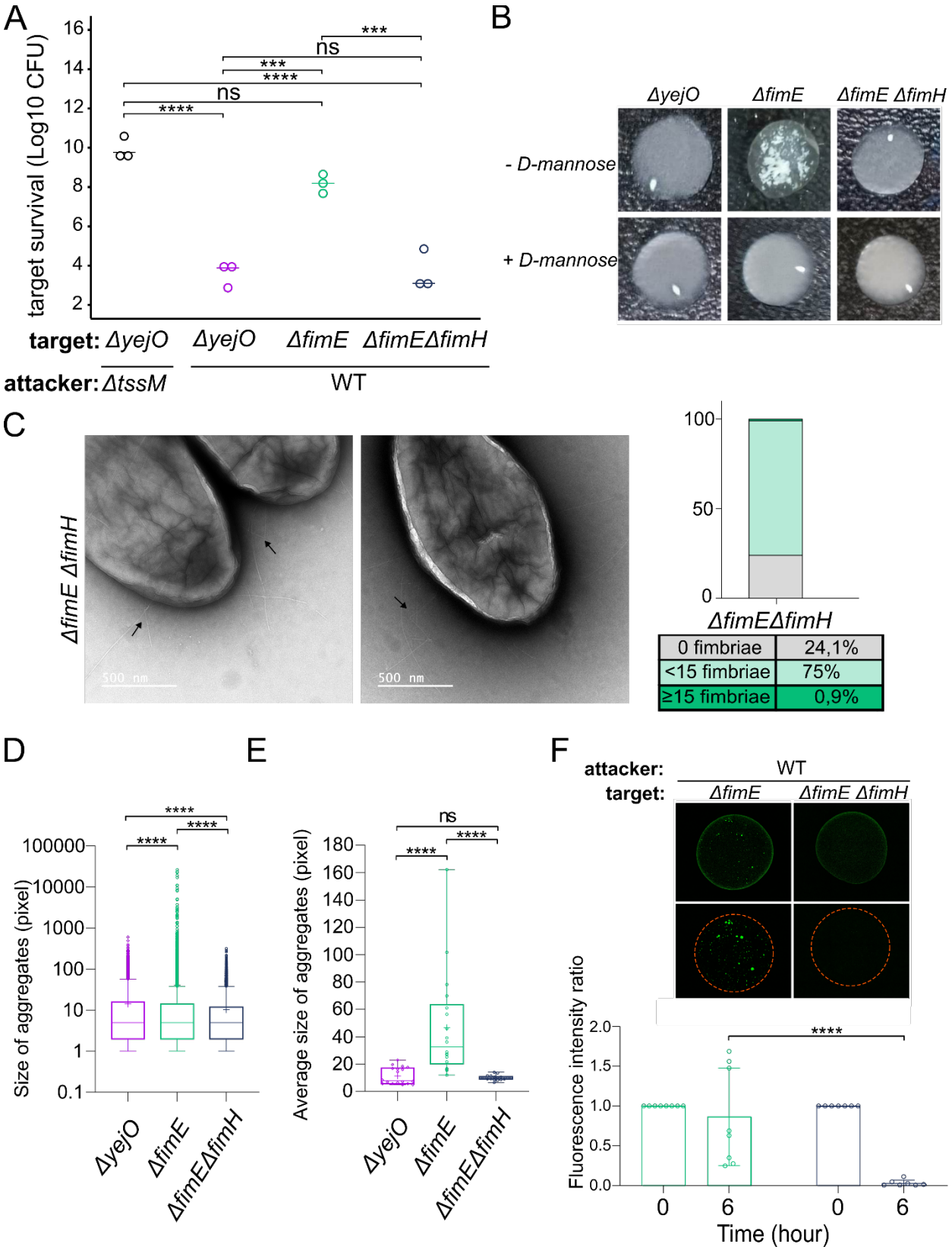

Supplementary Figure 3: (A) Interbacterial competition assay between *C. malonaticus 3267* WT or Δ*tssM* attacker and Δ*yejO*, Δ*fimE* and Δ*fimEfimH* target cells. Target survival

is presented in Log10 CFU. One-way Anova test was used followed by Tukey post-hoc test to determine statistical significance (ns=nonsignificant, ***p≤0.0005, ****p≤0.0001). Data represent three independent experiments. (B) Yeast agglutination assay with and without D-mannose as a competitive ligand to inhibit adhesion. A positive agglutination phenotype is observed for the Δ*fimE* mutant. A negative agglutination phenotype is characterized by a cloudy appearance of the mixture and observed for the Δ*fimEfimH* double deletion mutant. (C) Electron microscopy of fimbriated cells. Negatively stained preparation of a 24h stationary culture of *E. coli* BW25113 Δ*fimEfimH*, grown on LB agar plate. (D) Box plot of overall particles size of Δ*fimEfimH* mutant versus Δ*yejO* and Δ*fimE* mutants from fluorescence microscopy images. Box plots extend from the 5th to 95th percentiles. Cross: mean, crossing line: median. A nonparametric Kruskal Wallis test was performed followed by Dunn's post-hoc test to determine statistical significance (****p≤0.0001). (E) Box plots of the average size particles of each random point images. Box plots extend from min to max, showing all points. Cross: mean, crossing line: median. One-way Anova test was performed followed by Games-Howell post-hoc test with Welch's correction to determine statistical significance (ns=nonsignificant, ****p≤0.0001). (F) Confocal microscopy imaging of interbacterial killing using the same method as in Fig. 5. The killing rate was evaluated by assessing the total fluorescence inside the spot at 0h and 6h using ImageJ and compared with the initial fluorescence rate (at 0h). Unpaired t-test was performed to determine statistical significance using R (****p≤0.0001). Average ± s.d of n = 7-8 replicates.

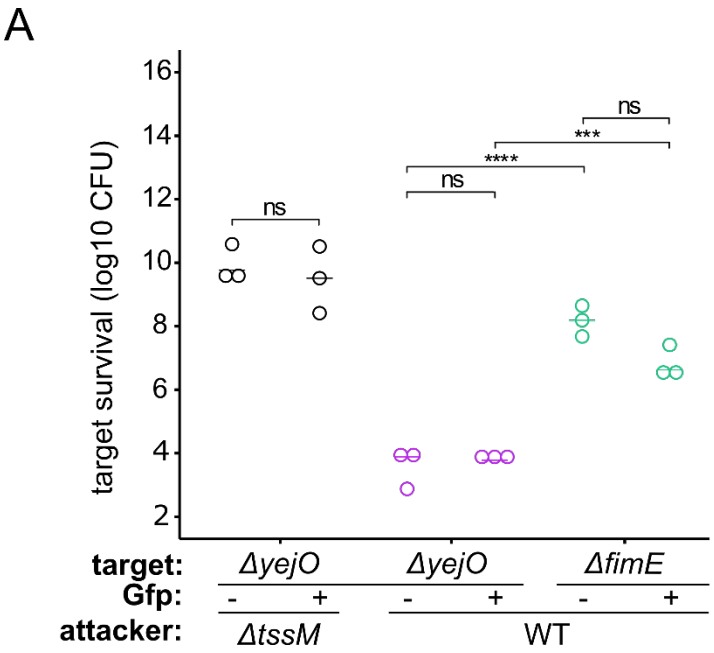

Supplementary Fig. 4: Interbacterial competition assay between *C. malonaticus 3267* WT or Δ*tssM* attacker and Δ*yejO* and Δ*fimE* target cells or Δ*yejO* GFP+ and Δ*fimE* GFP+ target cells. Target survival following interbacterial killing assay is presented in Log10 CFU. One-way Anova test was used followed by Tukey post-hoc test to determine statistical significance (ns=nonsignificant, ***p≤0.0005, ****p≤0.0001). Data represent three independent experiments.

Supplementary table 1:

Primers for gene deletion		
Gene	**F/R**	**sequences**
fimH	F	tcattctgtgacagagaaaaagtagccgaagatgacggttgccgacatcataacggttctgg
fimH	R	taaatggatgccctgcgtaagcggggcatttttcttcctgggtctgacagttaccaatgct
Primers for colony PCR verification		
Gene	**F/R**	**sequences**
fimH	F1	taccctgtttgctgtactgc
fimH	F2	ccatatcaccagctcaccg
fimH	R1	aagtcacgccaataatcgattg
fimH	R2	cggtgagctggtgatatgg

Supplementary table 2: summary of hits obtained following the HTIC assay.

No.	Disrupted gene	GO terms
present in three replicates		
1	*gnd*	pentose phosphate pathway
2	*tdcA*	transcriptional regulation
3	*glgC*	glycogen biosynthesis
5	*eutA*	protein repair
6	*yqhA*	response to hydrogen peroxide
present in two replicates		
7	*ppk*	polyphosphate biosynthesis
8	*ymcD*	membrane associated protein
9	*yjdE*	transmembrane transport
10	*yggM*	outer membrane/periplasm associated protein
11	*ldrD*	toxin-antitoxin system
12	*dicC*	Qin prophage; cell cycle/division
13	*tauB*	taurine transport
14	*sufI*	cell division
15	*sdhC*	aerobic respiration
16	*ynhF*	cellular response to hypoxia
17	*ypdB*	transcriptional regulation
18	*trpH*	rRNA processing
19	*ymgC*	biofilm formation
20	*yqfB*	pyrimidine nucleoside catabolism
21	*pspE*	thiosulfate sulfurtransferase activity
22	*kdpB*	potassium ion transport
23	*ygfS*	metal ion binding; putative oxidoreductase activity
24	*hokE*	DNA damage response
25	*yqhC*	transcriptional regulation
26	*tktB*	pentose phosphate pathway
27	*yfdI*	prophage genes and phage related functions
28	*helD*	DNA helicase activity
29	*gpmB*	glycolytic process
30	*hepA*	transcriptional regulation
31	*fruR*	transcriptional regulation: response to fructose
32	*ybiS*	peptidoglycan biosynthesis
33	*pepD*	proteolysis
34	*evgA*	phosphorelay signal transduction system; transcriptional regulation
35	*uvrB*	SOS response; DNA damage response
36	*ssuA*	transmembrane transport
37	*galK*	galactose metabolism
38	*yhfG*	Homologs of the E. coli Fic-FicA proteins act as toxin-antitoxin systems
39	*fimE*	DNA recombination; Type I fimbriae transcriptional regulation
40	*ybdO*	transcriptional regulation
41	*ygaD*	pyridine nucleotide synthesis
42	*yehB*	pilus assembly
43	*pdhR*	transcriptional regulation
44	*kdpE*	phosphorelay signal transduction system; transcriptional regulation
45	*stpA*	transcriptional regulation
46	*zntR*	transcriptional regulation
47	*cybB*	oxidoreductase activity
48	*ybaS*	glutamin metabolism; response to acidic pH
49	*cybC*	pseudogene